Electrocapillary Curves for the Hg/Ionic Liquid Interface

Andrzej Lewandowski, Tomasz Majkowski, and Maciej Galinski

Faculty of Chemical Technology, Poznań University of Technology, PL-60 965 Poznań, Poland

Reprint requests to A. L.; Fax: +48 61 662 571; E-mail: andrzej.lewandowski@put.poznan.pl

Z. Naturforsch. **64a,** 263 – 268 (2009); received April 15, 2008 / reveised September 2, 2008

Electrocapillary curves (surface tension γ as a function of the electrode potential E) for a series of room-temperature ionic liquids (RTILs) were measured using a mercury dropping electrode with the drop-weight (drop-volume) technique. The curves $\gamma = f(E)$ for the Hg/RTIL interface have one maximum and may be approximated with a polynomial of sixth-order. There are no 'humps' in the curves. The interfacial tension of the Hg/RTIL system changes with potential E in a monotonic way. The second derivative of $\gamma = f(E)$ leads to a polynomial of fourth order, indicating the capacitance of the Hg/RTIL interface. The potential of zero charge is within a relatively narrow range. The specific capacitance at the minimum is of the order 10 μF/cm^2.

Key words: Ionic Liquid; Electrocapillary Curve.

1. Introduction

Salts characterized by a low melting point, i. e. liquid at room-temperature or even below, form systems usually called room-temperature ionic liquids (RTILs) or simply ionic liquids (ILs). They may serve as solvents for chemical reactions as well as electrolytes in electrochemical devices. The first extensively studied RTIL was 1-ethyl-3-methyl-imidazolium tetrachloroaluminate ($EtMeImAlCl_4$). However, ILs containing the $AlCl_4^-$ anion are easily hydrolyzed. Non-chloroaluminate RTILs, resistant to moisture, have been developed and studied extensively during the last decade [1 – 4]. Electrochemical double-layer capacitors (EDLCs), based on carbon materials having a very high surface area, have been developed at the same time as energy-storage devices with very promising results. Various liquid electrolytes, both aqueous and non-aqueous, as well as polymer electrolytes have been applied [5 – 17]. There are also reports available, which describe attempts to apply ILs in EDLCs [18 – 26]. In [5 – 26] devices prepared from different types of activated carbon (AC) are described. The specific capacitance of the AC/electrolyte interface has been expressed versus the carbon total mass (F/g) or versus the total carbon surface estimated from the BET isotherm (μF/cm^2). The wettability as a function of the potential is interesting from the point of view of actuators as well as of carbon-based double-layer capacitors. The degree of wetting is described by the angle at which the liquid/vapor interface meets the solid/liquid interface. The term 'electrowetting', in contrast to the term 'wetting', is usually used to describe a system in which the electron-conducting electrode and ion-conducting fluid (electrolyte) are separated by a layer of an insulating dielectric material. While the electrowetting concept is rather related to the three-phase solid-liquid-gas system, the electrocapillary curve describes the change in the two-phase electrode/electrolyte interface. There are only a few publications about measurements of the double-layer capacitance at a geometrically defined electrode/electrolyte surface, apart from a paper on ILs based on the chloroaluminate ion [27] and a work on the specific capacitance for glassy carbon (GC), mercury and a commercial carbon as electrode materials, and four ILs based on the 1-ethyl-3-methyl-imidazolium cation [28]. The differential capacitance at the electrode/IL interface (Pt, Au) was measured for 18 ILs by directly applying chronoamperometry [29]. The double-layer capacitance at the Pt/IL and Au/IL interface was at the level of 1 – 8 μF/cm^2. The electrocapillary curve (mercury dropping time as a function of potential) was measured in 1-ethyl-3-methyl-imidazolium tetrafluoroborate and 1-propyl-3-methyl-imidazolium tetrafluoroborate [30, 31]. The general aim of the present work was to determine electrocapillary curves at the Hg/IL interface for a number of room-temperature ILs, using the drop-weight (drop-volume) technique.

2. Experimental

2.1. Chemicals

Cryptand 222 (4,7,13,16,21,24-hexaoxa-1,10-diazabicyclo[8.8.8]hexacosane) and silver perchlorate were obtained from Merck. Ionic liquids (Table 1): diethyl-methyl-sulfonium bis(trifluoromethanesulfonyl)imide ($Et_2MeSNTf_2$), triethyl sulfonium bis(trifluoromethanesulfonyl)imide (Et_3SNTf_2), 1-ethyl-3-methyl-imidazolium bis(trifluoromethanesulfonyl)imide ($EtMeImNTf_2$), 1-ethyl-3-methyl-imidazolium triflate (EtMeImOTf) (all from Iolitech, Germany); 1-ethyl-3-methyl-imidazolium tetrafluoroborate ($EtMeImBF_4$), 1-butyl-3-methyl-imidazolium triflate (BuMeImOTf) (from Merck); 1-butoxymethyl-imidazolium lactate (racemate) [C_4OmImLact(DL)], 1-butoxymethyl-imidazolium L-lactate [C_4OmImLact(L)], 1-methyl-3-*H*-imidazolium L-lactate [MeHImLact(L)], 1-methyl-3-*H*-imidazolium lactate (racemate) [MeHImLact (DL)] (all from the J. Pernak group, Poznan University of Technology, Poznan, Poland [32, 33]), were dried before measurement under vacuum at ca. 40 °C for 24 h. *N*-Butyl-*N*-methyl-pyrrolidinium bromide (BuMePyrrBr) was synthesized from *N*-methyl-pyrrolidine (Aldrich) and bromopropane (Aldrich) in chloroform. BuMePyrrBr was purified by crystallization in 2-propanol (P.O.Ch., Poland); after addition of tetrahydrofurane (P.O.Ch.) white crystals of BuMePyrrBr were precipitated. 1-Butyl-3-methyl-pyrrolidinium bis(trifluoromethanesulfonyl)imide ($BuMePyrrNTf_2$) was obtained from BuMePyrrBr by metathesis with lithium bis(trifluoromethanesulfonyl) imide (Fluka) in aqueous solution. The IL was dried under vacuum at 50 °C for 24 h. The water content, analyzed with a Karl Fischer titrant (Aldrich, Cat. No: 22,120-1), was below the detection limit.

2.2. Measurements

All tested ILs were deaerated with nitrogen before measurement. Electrocapillary curves were measured with a dropping mercury electrode with constant height of the mercury head. The potential of the mercury electrode was adjusted with the use of an EP20A potentiostat (Elpan, Poland), using a platinum counter electrode (1 cm^2) and a cryptate reference electrode, composed of a silver wire immersed in a solution of $AgClO_4$ (0.01 M) and cryptand 222 (0.1 M) in acetonitrile: (Ag/Ag^+ 0.01 M, 222 0.1 M, AN). The solution was contained in a glass tube with a glass frit at the end. The potential of the electrode is stabilized by the equilibrium of the Ag^+ ion complexation with cryptand 222, similarly to the potential stabilization by the ionic product of slightly soluble salts, used in aqueous electrodes of the second kind [34, 35]. The potential of the (Ag/Ag^+ 0.01 M, 222 0.1 M, AN) electrode, used in this work, is −0.464 V versus the (Ag/Ag^+ 0.01 M, AN) electrode and −0.177 V versus the aqueous saturated calomel electrode. The glass capillary had an outer diameter of 6.04 mm and an inner diameter of 0.0457 mm.

Table 1. List of symbols and abbreviations.

R	Radius of the mercury drop
r	Radius of the capillary
γ	Surface tension
q	Surface charge density
C	Electrical capacitance
d	Density
E	Potential
$Et_2MeSNTf_2$	Diethyl-methyl-sulfonium bis(trifluoromethanesulfonyl)imide
$EtMeImNTf_2$	1-Ethyl-3-methyl-imidazolium bis(trifluoromethanesulfonyl)imide
BuMeImOTf	1-Butyl-3-methyl-imidazolium triflate
$BuMePyrrNTf_2$	1-Butyl-3-methyl-pyrrolidinium bis(trifluoromethanesulfonyl)imide
$OctPyBF_4$	*N*-Octyl-pyridinum tetrafluoroborate
Et_3SNTf_2	Triethyl sulfonium bis(trifluoromethanesulfonyl)imide
EtMeImOTf	1-Ethyl-3-methyl-imidazolium triflate
$EtMeImBF_4$	1-Ethyl-3-methyl-imidazolium tetrafluoroborate
C_4OmImLact(DL)	1-Butoxymethyl-imidazolium lactate (racemate)
C_4OmImLact(L)	1-Butoxymethyl-imidazolium L-lactate
MeHImLact(L)	1-Methyl-3-*H*-imidazolium L-lactate
MeHImLact(DL)	1-Methyl-3-*H*-imidazolium lactate (racemate)

If the mercury drop, spreading out from the internal bore of the tip (of radius r), is at equilibrium, the surface tension force $F = 2\pi r\gamma$ is counterbalanced by the gravity force $F = mg$, where m is the mercury drop mass, $g = 9.81$ m/s^2, and r is the capillary radius. The displacement force (equal to the weight of the IL displaced by the mercury drop of radius R) acts against the gravity, and hence the surface tension may be approximated by the following equation:

$$\gamma = (d_{Hg} - d_{IL})g\frac{2R^3}{3rf}, \qquad (1)$$

where d_{Hg} and d_{IL} stand for the density of mercury and of the IL, respectively, f is a correction factor for the non-ideally spherical shape of the drop and the drop residue. The shapes of drops were observed with the use of a digital camera with 50× magnification. The drops were measured at least ten times and the mean value was used to calculate the surface tension at each potential.

3. Results and Discussion

A typical picture of a mercury drop recorded just before falling from the capillary is shown in Fig. 1, indicating a typical diameter of the mercury drop of ca. 1 mm ($R \approx 5 \cdot 10^{-4}$ m). The corresponding volume V, calculated assuming an ideally spherical shape of the drop, is ca. $5 \cdot 10^{-10}$ m^3. The correction factor f appearing in (1) should be a function of the dimensionless ratio of the dropping-tip radius to the cube root of the drop volume $(r/\sqrt[3]{V})$ [36]. Hence, the $r/\sqrt[3]{V}$ ratio was typically of the order $2.3 \cdot 10^{-5}\ \mathrm{m}/\sqrt[3]{5 \cdot 10\ \mathrm{m}^3} \approx 0.029$. The value of the factor f, for a non-wetting liquid such as mercury, may be estimated on the basis of the experimentally determined $f = f(r/\sqrt[3]{V})$ curve, available in the literature [37]. In a series of experiments, the mercury drop was falling from glass capillaries of different size in nitrogen. The f value increased monotonically with decreasing $r/\sqrt[3]{V}$ value up to $f = 1$ at $r/\sqrt[3]{V} = 0$. At such a small $r/\sqrt[3]{V}$ value as 0.029, the correction factor f may be expected to be rather close to unity. Capillary curves (non-corrected surface tension as a function of the potential) are shown in Fig. 2 [all data expressed versus the (Ag/Ag$^+$ 0.01 M, 222 0.1 M, AN) reference]. The curves have a rather regular, classical shape, with one maximum and without any additional maximum, minimum, or hump. The surface tension between the electrolyte and the electron conductor (electrode) at zero electric field γ_0 is perturbed to a new γ value by applying a voltage E across the electrode/electrolyte interface and may be approximated by the equation

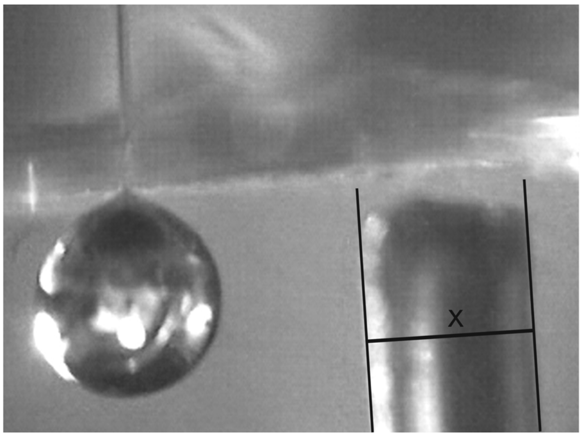

Fig. 1. Mercury drop just before falling and the scaling rod ($x = 0.96$ mm).

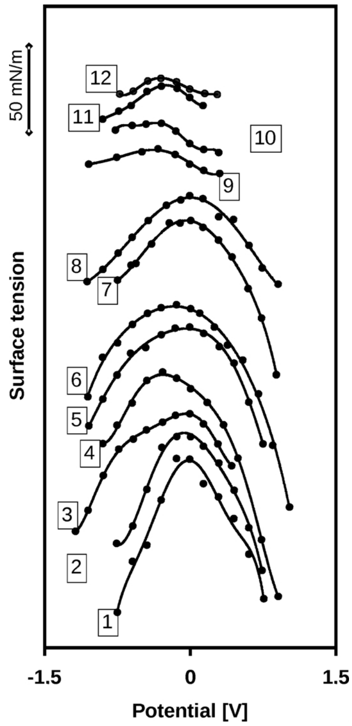

Fig. 2. Electrocapillary curves for the Hg/IL interface. The ILs are numbered as follows: 1, $Et_2MeSNTf_2$; 2, Et_3SNTf_2; 3, $EtMeImNTf_2$; 4, EtMeImOTf; 5, $EtMeImBF_4$; 6, BuMeImOTf; 7, $BuMePyrrNTf_2$; 8, $OctPyBF_4$; 9, $C_4OmImLact(DL)$; 10, $C_4OmImLact(L)$; 11, MeHImLact(L); 12, MeHImLact(DL).

$$\gamma = \gamma_0 - \frac{CE^2}{2}, \tag{2}$$

where C is the capacitance of the electrode/electrolyte interface, $\varepsilon\varepsilon_0/d$, for a dielectric material of thickness d and permittivity ε; ε_0 is the vacuum permittivity. This is the equation for a parabola, describing a system characterized by a constant capacitance C of the double layer, independent of the applied voltage E. However, the $\gamma = f\ (E)$ curves are not ideal parabolic and they are described by an empirical polynomial of the sixth-order:

$$\gamma = \sum_{i=0}^{i=6} a_i E^i. \tag{3}$$

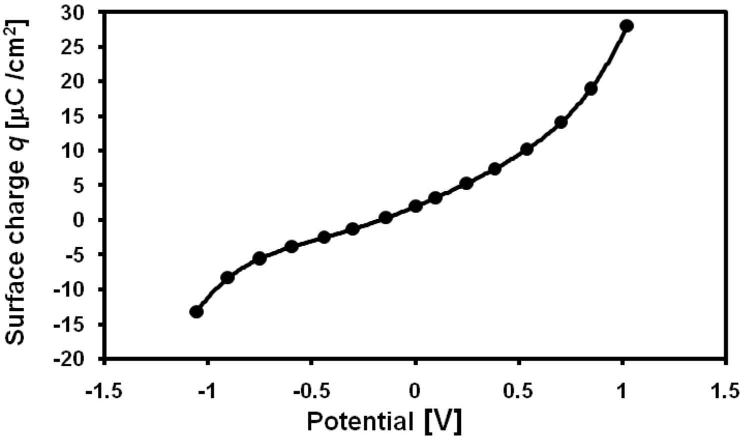

Fig. 3. Surface charge density for the Hg/BuMeImOTf interface.

Table 2. Potential of the electrocapillary curve maximum [expressed vs. potential of the (Ag/Ag$^+$ 0.01 M, 222 0.1 M AN) reference electrode] as well as the corresponding interfacial tension for the Hg/IL interface. $T = 25$ °C.

No.	IL	E [V]	γ_{max} [N/m]
1	$Et_2MeSNTf_2$	0.00	0.37
2	Et_3SNTf_2	−0.05	0.37
3	$EtMeImNTf_2$	−0.04	0.36
4	EtMeImOTf	−0.28	0.36
5	$EtMeImBF_4$	−0.05	0.35
6	BuMeImOTf	−0.17	0.34
7	$BuMePyrrNTf_2$	−0.03	0.35
8	$OctPyBF_4$	−0.05	0.34
9	C_4OmImLact(DL)	−0.36	0.33
10	C_4OmImLact(L)	−0.38	0.34
11	MeHImLact(L)	−0.30	0.35
12	MeHImLact(DL)	−0.30	0.34

Potentials of zero charge (PZC, maximum of curves) are listed in Table 2. It can be seen that the PZC values are within a relatively narrow range between ca. 0 and −0.38 V [versus the (Ag/Ag$^+$ 0.01 M, 222 0.1 M, AN) reference electrode]. The four lactates are characterized by the lowest PZC values (−0.30 to −0.38 V). Similarly, ILs containing triflate anions show PZC values at the level of −0.28 and −0.17 V, while the sulfonium-based ILs show the highest potentials of PZC appearance, close to 0 V. This is also characteristic for the ILs based on lactate anions, namely that the electrocapillary curves are relatively flat in comparison to the remaining compounds under study. All this may suggest that anions are mainly responsible for the structure of the double layer formed at the Hg/IL interface. The interfacial tension at PZC is at the relatively constant level of (0.34 ± 0.03) Nm^{-1}.

The double layer formed at the electrode/electrolyte interface (both phases contain mobile charges) may be discussed taking into account two mutual interrelated aspects: electrical and structural ones. Especially, the specific adsorption of charged or neutral species from the liquid solution at the electrode surface may strongly influence the electric properties of the interface. ILs, being molten salts, consist only of ions as well as their charged and neutral aggregates. The possible structural aspects of the electrode/IL electrified interface is difficult to discuss since the common model of ILs, assuming that the system consists entirely of ions, causes a conceptual problem regarding the distinction of individual ionic species present in the system. Ions of opposite sign are close and form aggregates, which may be regarded as electrically neutral species. In addition, one may expect different ion-ion interactions in different ILs, leading to the formation of different ionic species (or ionic aggregates). Computer simulation studies [38] as well as in situ STM experimental investigation [39] of the electrode/IL interface can be found in the literature. It has been suggested that the electrode induces crystallinity in adjacent layers of the molten salt and that the excess charge is due to anions occupying cationic sites (and vice versa). The computer simulation of the boundary formed between molten KCl (above the melting point and near zero pressure) and rigid, smooth walls (electrode) showed charge separation [38]. Such a result was obtained both for a unperturbed system as well as with externally applied field (10^7 V/cm). Recently the adsorption of hexafluorophosphate anions (PF_6^-) on Au(111) from a 1-butyl-3-methyl-imidazolium hexafluorophosphate room-temperature melt was analyzed experimentally by scanning tunnelling microscopy [39]. The adsorption of PF_6^- anions was observed. The structure of the ordered layers changed with the potential of the electrode. Such structural changes within the double layer

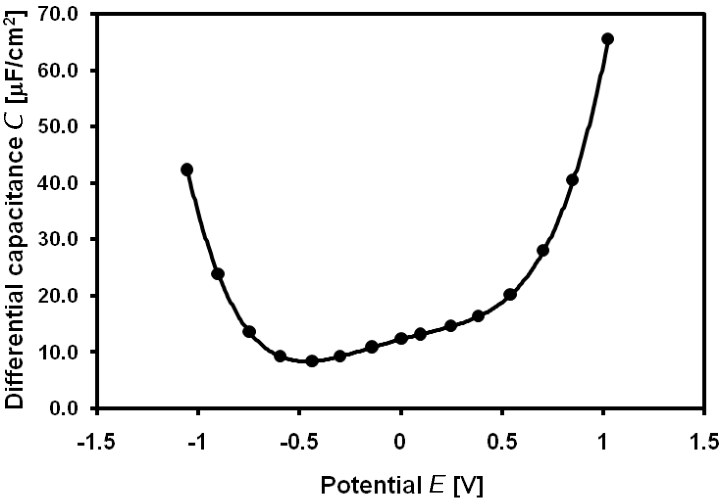

Fig. 4. Differential capacitance for the Hg/BuMeImOTf interface.

may be responsible for the deviations of the electrocapillary curves from the perfect parabolic shape, obtained assuming a constant capacitance of the double layer [see (1)].

The change in the Hg/IL interfacial tension with the potential according to the Lipmann relation is equal to the surface charge density q:

$$q = -\frac{\partial \gamma}{\partial E} = -\sum_{i=1}^{i=6} i a_i E^{i-1}. \tag{4}$$

The derivative (4) leads to a polynomial of fifth-order. The charge cumulated at the Hg/IL interface, calculated from the polynomial, has an almost linear dependence on the potential E. An example is shown in Fig. 3 for the IL BuMeImOTf. The capacitance may be calculated as the second derivative, which leads to a polynomial of fourth-order:

$$C = -\frac{\partial^2 \gamma}{\partial E^2} = -\sum_{i=2}^{i=6} i(i-1) a_i E^{i-2}. \tag{5}$$

An example for a typical curve $C = f\ (E)$ is shown in Figure 4. The minimum differential capacitance is of the order 10 μF/cm^2. This is comparable to the value reported for the Hg/PrMeImBF$_4$ interface [31]. It is difficult to compare the results obtained in the present work with some other solvent-free systems, since systematic direct measurements of electrocapillary curves at the dropping mercury electrode have not been done in high-temperature ILs due to evaporation of mercury in the temperature ranges of classical salts' liquidity. However, there are data for high-temperature molten metal electrodes, such as Bi, Ag, Tl, Sn, or Pb, in high-temperature molten salts, such as NaCl or NaCl + KCl [40]. In these systems the electrocapillary curves, as well as differential capacitance curves, have a parabolic shape, and the minimum capacitance is of the order 20 – 75 μF/cm^2. In the case of electrode metals such as Ag, Tl, and Sn, there is a flat region in the $C = f\ (E)$ curve on the more negative potential region. The origin of this phenomenon has not yet been understood [40]. It has also been established that $C_{\min}$ occurs close to the potential of zero charge and is rather independent of the nature of the electrode metal.

The electrochemical stability window of room-temperature ILs based on BF$_4^-$, NTf$_2^-$ or OTf$^-$ anions is usually broad, as high as 4 – 6 V [4]. Imidazolium-based RTILs with lactate anions show a considerably lower stability range, but still at the level of 2.3 V [41]. However, the shape of the $C = f\ (E)$ curve at higher applied voltages (ca. ±1 V) may suggest possible Faradaic reactions which may take place at the Hg/RTIL interface.

4. Conclusions

1. Electrocapillary curves for a series of room-temperature ILs show a regular shape with one maximum. There are no 'humps' in the $\gamma = f\ (E)$ curves. The changes of the interfacial tension with potential E are monotonic and very similar at both sides of the maximum.
2. Electrocapillary curves can be approximated by a polynomial of sixth-order.
3. The minimum value of the capacitance C, estimated from the $C = f\ (E)$ curves, is at the

level of ca. 10 μF/cm^2. For comparison, the literature data for high-temperature molten metal electrodes, such as Bi, Ag, Tl, Sn, or Pb, in high-temperature molten salts, such as NaCl or NaCl + KCl, indicates a minimum capacitance of the order of 20 – 75 μF/cm^2.

Acknowledgements

This work was supported by grant DS31-128/07. The gift of sulfonium ILs (Iolitech, Germany) and ILs containing lactate anions (Prof. J. Pernak) is gratefully acknowledged.

[1] T. Welton, Chem. Rev. **99**, 2071 (1999).
[2] M. J. Earle and K. R. Seddon, Pure Appl. Chem. **72**, 1391 (2000).
[3] P. Wasserscheid and W. Keim, Angew. Chem., Int. Ed. **39**, 3772 (2000).
[4] M. Galinski, A. Lewandowski, and I. Stępniak, Electrochim. Acta **51**, 5567 (2006).
[5] B. E. Conway, Electrochemical Supercapacitors, Kluwer Academic Plenum Publisher, New York 1999.
[6] R. Koetz and M. Carlen, Electrochim. Acta **24**, 2483 (2000).
[7] J.-C. Lassegues, J. Grondin, T. Becker, L. Servant, and M. Hernandez, Solid State Ionics **77**, 311 (1995).
[8] D. Qu and H. Shi, J. Power Sources **74**, 99 (1998).
[9] A. Lewandowski, M. Zajder, E. Frąckowiak, and F. Béguin, Electrochim. Acta **46**, 2777 (2001).
[10] F. Beck, M. Dolata, E. Grivei, and N. Probst, J. Appl. Electrochem. **31**, 845 (2001).
[11] M. Endo, J. Y. Kim, T. Takeda, T. Maeda, T. Hayashi, K. Koshiba, H. Hara, and M. S. Dresselhaus, J. Electrochem. Soc. **148**, A1135 (2001).
[12] C. Arbizzani, M. Mastragostino, and F. Soavi, J. Power Sources **100**, 134 (2001).
[13] J. Gamby, P. L. Taberna, P. Simon, J. F. Fauvarque, and M. Chesneou, J. Power Sources **101**, 109 (2001).
[14] J. Bispo-Fonseca, J. Aggar, C. Sarrazin, P. Simon, and J. F. Fauvarque, J. Power Sources **79**, 238 (1999).
[15] L. Bonnefoi, P. Simon, J. F Fauvarque, C. Sarrazin, and A. Dugast, J. Power Sources **79**, 37 (1999).
[16] A. Lewandowski and M. Krzyzanowski, Electrochim. Acta **48**, 1325 (2003).
[17] A. Lewandowski, M. Galinski, and M. Krzyzanowski, Solid State Ionics **158**, 367 (2003).
[18] M. Watanabe, S. Yamada, and N. Ogata, Electrochim. Acta **40**, 2285 (1995).
[19] J. Fuller, A. C. Breda, and R. T. Carlin, J. Electrochem. Soc. **144**, L67 (1997).
[20] J. Fuller, A. C. Breda, and R. T. Carlin, J. Electroanal. Chem. **459**, 29 (1998).
[21] M. Doyle, S. K. Choi, and G. Proulx, J. Electrochem. Soc. **147**, 34 (2000).
[22] A. Noda and M. Watanabe, Electrochim. Acta **45**, 1265 (2000).
[23] A. Lewandowski and A. Swiderska, Solid State Ionics **161**, 243 (2003).
[24] A. Lewandowski and M. Galiński, Phys. Chem. Solids **65**, 281 (2004).
[25] A. Lewandowski and A. Swiderska, Solid State Ionics **169**, 21 (2004).
[26] A. Lewandowski and A. Swiderska, Polish J. Chem. **78**, 1371 (2004).
[27] R. J. Gale and R. A. Osteryoung, Electrochim. Acta **25**, 1527 (1980).
[28] C. Nanyundiah, S. F. McDevitt, and V. R. Koch, J. Electrochem. Soc. **144**, 3392 (1997).
[29] A. Lewandowski, M. Galiński, and S. R. Krajewski, Z. Naturforsch. **62a**, 187 (2007).
[30] M. M. Islam, M. T. Alam, T. Okajima, and T. Ohsaka, J. Phys. Chem. **111B**, 12849 (2007).
[31] M. T. Alam, M. M. Islam, T. Okajima, and T. Ohsaka, Electrochem. Commun. **9**, 2370 (2007).
[32] J. Pernak and I. Goc, Polish J. Chem. **77**, 975 (2003).
[33] J. Pernak, P. Chwala, and A. Syguda, Polish J. Chem. **78**, 539 (2004).
[34] A. Lewandowski, A. Szukalska, and M. Galinski, New J. Chem. **19**, 1259 (1995).
[35] A. Lewandowski, M. Galinski, and M. Osinska, Patent P-380534 (2007).
[36] A. W. Adamson and A. P. Gast, Physical Chemistry of Surfaces, 6th Ed., Wiley-Interscience, New York 1997.
[37] M. C. Wilkinson and M. P. Aronson, J. Chem. Soc. Faraday Trans. 1 **69**, 474 (1973).
[38] D. M. Heyes and J. H. R. Clarke, J. Chem. Soc. Faraday Trans. 2 **77**, 1089 (1981).
[39] G.-B. Pan and W. Freyland, Chem. Phys. Lett. **427**, 96 (2006).
[40] M. A. V. Devanathan and B. V. K. S. R. A. Tilak, Chem. Rev. **65**, 635 (1965).
[41] S. Krajewski, PhD Thesis, Poznan University of Technology 2006.